

Effect of Recirculation Channel on Aerodynamic Performance of a Single-Stage Transonic Axial Compressor

Cong-Truong Dinh

Hanoi University of Science and Technology - No. 1, Dai Co Viet, Hai Ba Trung, Ha Noi, Viet Nam

Received: December 12, 2019; Accepted: June 22, 2020

Abstract

This paper investigates the effects of recirculation channel on the performance of a single-stage transonic axial compressor, NASA Stage 37, such as pressure ratio, adiabatic efficiency, and operating range. Numerical analysis was conducted by solving three-dimensional steady Reynolds-averaged Navier-Stokes equations with the k -epsilon turbulence model. The recirculation channel bled the high-pressure flow from the stator shroud domain and injected it into the rotor tip clearance domain to increase the aerodynamic performance. The locations and widths of the injection and bleed ports were selected as parameters for the study to find the optimum recirculation channel design. The results indicated that, in general, the stall margin and operating range were significantly extended by from 0.45% to 2.38%, and from 3.72% to 12.7%, respectively, as compared to the performance of the smooth case without recirculation channel.

Keywords: Single-stage transonic axial compressor, recirculation channel, reynolds-averaged navier-stokes analysis, total pressure ratio, adiabatic efficiency, stall margin, stable range extension.

1. Introduction

Complex flow phenomena at the rotor blade tip region have a significant effect on the performance of axial compressors. Many studies have applied different methods, such as casing grooves [1 - 5], and flow rejection/injection [6 - 10], to improve the performance of the axial compressor.

Weichert et al. [6] demonstrated stall margin improvements between 2.2 and 6.0% and efficiency penalties between 0 and 0.8% in a single-stage axial compressor with the use of different rotor self-regulating loop positions. Strazisar et al. [7] conducted experiments with six recirculation bridges installed in a single-stage compressor rotating at 70% and 100% design speed. The results showed an increase in stalling flow coefficient of 6% and 2%, respectively. Hathaway [8] employed CFD (Computational Fluid Dynamics) simulation to examine the effects of self-recirculating casing treatment on axial compressor performance. They found that the operating range increased by 60% for a moderate-speed compressor, and at least by 125% for a transonic compressor. Dinh et al. [9] added an injector on the stator shroud. It was concluded that, with the appropriate injector geometry and injection mass flow rate, the model enhanced the compressor efficiency and delayed stall.

Dinh et al. [10] also designed a circumferential feedback channel to recirculate the flow at the rotor tip region of a transonic axial compressor. The effects of eight geometric parameters of the channel were examined and it was concluded that the channel reduced the compressor efficiency, near-stall pressure ratio, and increased the stable range of the compressor. This study was conducted based on this work to examine the effects of the channel on the same compressor when the bleed port was put in the stator domain.

2. Numerical Analysis

2.1. Description of Geometry

The single-stage transonic axial compressor investigated in this work was NASA Stage 37 with 36 blades of Rotor 37 at a rotational speed of 17185.7 rpm (100% design speed) and 46 blades of Stator 37 [11]. The values of the tip clearance for the rotor and stator blades were respectively 0.04 cm at the rotor shroud and 0.0762 cm at the stator hub. At the design rotational speed of 17185.7 rpm, the maximum adiabatic efficiency was 84.00% at a mass flow rate of 20.74 kg/s, the maximum pressure ratio 2.00 at 19.6 kg/s, and the choking mass flow rate at 20.93 kg/s. The reference temperature and pressure were 288.15 K and 101,325 Pa, respectively.

The geometry of the single-stage compressor and the recirculation channel was generated using ANSYS 19.1 [12] as shown in Fig.1. The compressor geometry and definition of geometric parameters of the circumferential recirculation channel are shown in

* Corresponding author: Tel.: (+84) 934.638.035
Email: truong.dinhcong@hust.edu.vn

Fig.2. The angles: α and β indicate the injection and bleed angles, respectively, and their reference values are often 45° . The locations of the injection port (L_R) in the rotor domain and bleed port (L_S) in the stator domain are respectively measured from the leading edge of the rotor and the stator blade at the shroud, and their respective widths are represented by W_R and W_S . The values L_R , W_R , L_S , and W_S are accordingly non-dimensionalized by the chord lengths of the rotor and stator blades (C_R and C_S , which are the chord length of rotor and stator blades at the shroud surface, respectively). The reference design of the recirculation channel and its parameters are shown in Tab. 1. In this study, L_R , L_S , W_R and W_S were varied as shown in Tab. 2 to examine effects of these parameters on the aerodynamic performance of the compressor.

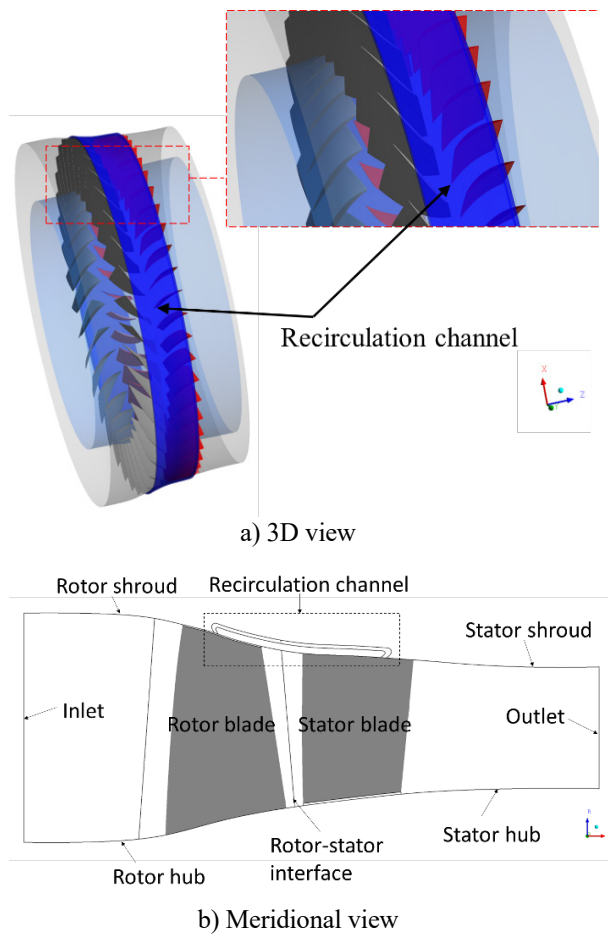


Fig. 1. Stage 37 with recirculation channel

2.2. Numerical method

DesignModeler® was used to design the rotor and stator blade and the recirculation channel, then the blades were meshed in TurboGrid®, and the channel by ICEM CFD. CFX-Pre, CFX-Solver, and CFD-Post were employed to set up the simulation,

solve the 3D RANS (Reynolds-averaged Navier-Stokes) equations, and process the results. Hexahedral grids were used to mesh the computational domain with O-type grids near the blade surfaces, and H/J/C/L-type grids in other regions of the rotor and stator as shown in Fig. 3.

The working fluid was assumed to be air ideal gas. Relative static pressure boundary condition was set at both the domain inlet (the stator inlet) and the domain outlet (the stator outlet). The value of static pressure at the inlet was kept at 0 Pa while the value at the outlet was changed from 0 Pa to the value where maximum pressure ratio was achieved with increments of 100 Pa and 10 Pa to find the maximum adiabatic efficiency point and maximum pressure ratio point, respectively.

Table 1. Reference design of the recirculation channel

Parameter	Ref. value
α ($^\circ$)	45
β ($^\circ$)	45
H/τ (%)	300
L_R/C_R (%)	40
L_S/C_S (%)	70
W_R/C_R (%)	5
W_S/C_S (%)	5

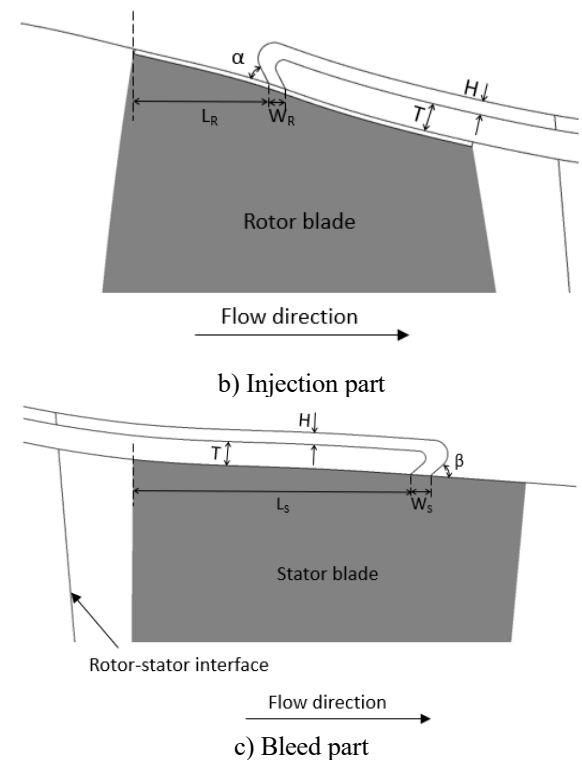


Fig. 2. Geometry of recirculation channel

Table 2. Ranges for parametric study

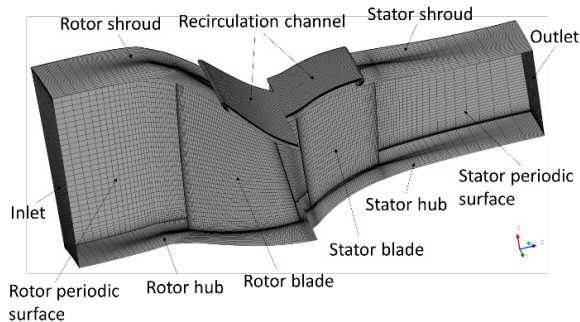
Parameter	Range
L_R/C_R (%)	20 – 70
L_S/C_S (%)	40 – 150
W_R/C_R (%)	1 – 7
W_S/C_S (%)	1 – 7

A turbulence intensity of 5% was specified at the rotor inlet. The adiabatic smooth wall condition was applied at all the walls in the domain such as the blade surface. The periodic surfaces of the domain were connected by rotational periodic condition, and the frozen rotor method was used to connect the interfaces of the rotor and stator domain, the injection and bleed parts of the channel, and the channel and the rotor domain. All the interfaces were connected by General Grid Interface (GGI). The two-equation $k-\epsilon$ turbulence model [13] with a scalable wall function was used with y^+ value of the first nodes near the walls ranging from 20 to 100. The reliability of the method was confirmed by Dinh et al. [9].

The performance parameters of a single-stage transonic axial compressor, NASA stage 37 in this research were the total pressure ratio (PR), adiabatic efficiency (η), stall margin (SM) and operating range (SRE), which were presented by Dinh et al. [9].

Table 3. Mesh and computing time in smooth case

Mesh	Grid number	Time (h)
Mesh 1	336,236	0.6
Mesh 2	590,080	2.5
Mesh 3	914,188	6
Mesh 4	1,200,000	9


Fig. 3. Mesh of the computational domain

The peak and near-stall conditions were defined as the points where the maximum adiabatic efficiency and maximum total pressure ratio are achieved, respectively. The stall margin is a measure of how far the peak point is to near-stall point. The stable range extension is the increase in the stable operating range

(between choke and near-stall) of the case with recirculation channel as compared to the smooth case.

3. Results and discussion

Four different meshes (Tab.3) were created to examine the effect of grid number on the results. Fig.4 shows the predicted performance curves of the four meshes. When the number of grids were kept increasing from Mesh 2 to Mesh 4, there were very small differences in the results; however, the average computational time for each pressure point increased at least 3 hours from one mesh to the other (Tab.3). Due to limited computational resources and its acceptable results, therefore, Mesh 2 was chosen as the optimum mesh for further calculations.

To validate the chosen mesh, the predicted performance curves were compared with experimental data reported by Reid and Moore [11]. Fig.5 shows a close match between the curves and the data; there were relatively small 0.18% and 0.23% errors in the adiabatic efficiency and the pressure ratio at operating condition, respectively; the predicted normalized mass flow rate at near-stall condition was 93.85%, also very close to the reported datum (93.65%).

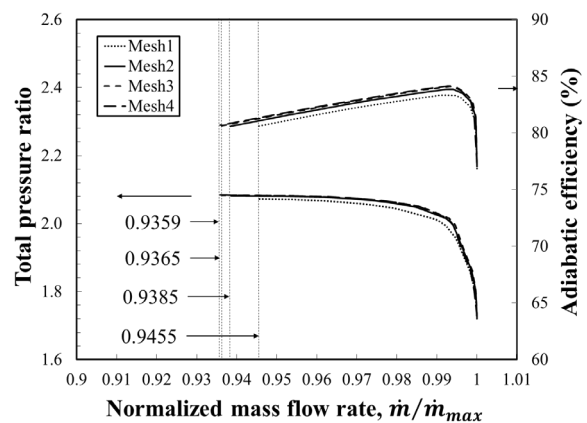

Fig. 4. Grid-dependency test for smooth case

Fig.6 shows the variations of the adiabatic efficiency with respect to the four geometric parameters. In general, the adiabatic efficiency decreased in all situations. When the injection port was moved along the casing, the efficiency penalty decreased from 0.66% at $L_R/C_R = 20\%$ to the minimum value of 0.43% at $L_R/C_R = 50\%$, and then increased again to 0.52% at $L_R/C_R = 70\%$. Whereas, the decrease in efficiency remained around 0.49% when the bleed port was moved along the shroud. As for the effects of the widths of the two ports, the narrower the ports were, the less the efficiency penalty was.

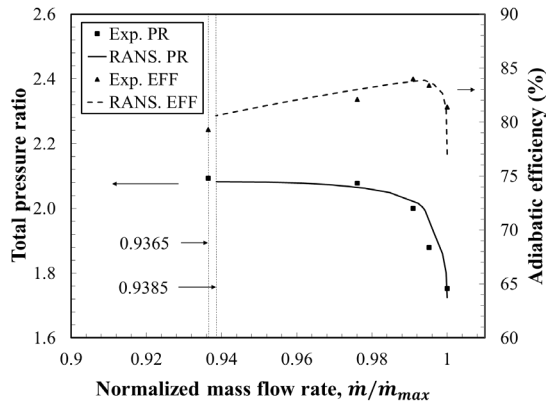


Fig. 5. Mesh validation for smooth case

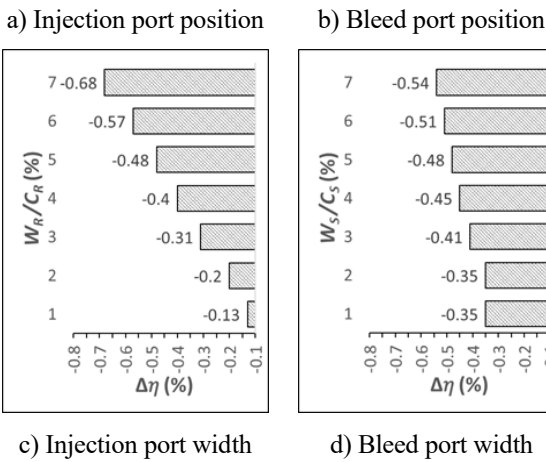
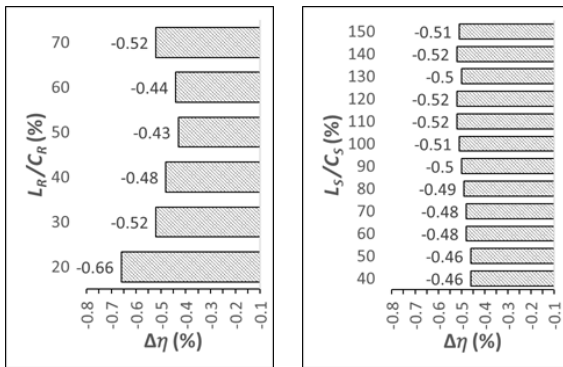


Fig. 6. Effect on adiabatic efficiency

The effect of the four geometric parameters on the stable operating range of the compressor is illustrated in Fig.7. The position of the injection port had a relatively small effect on the operating range with the SRE values of the case all smaller than 8% (Fig.7a). As for the effect of the bleed port position and the widths of the two ports (Fig.7(b, c)), the increase in the operating range was in general from 7.5% to 12.7%, which the maximum value of 12.7% at $L_S/C_S = 60\%$.

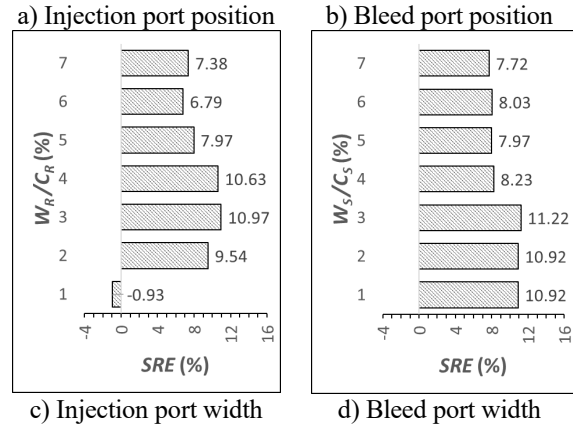
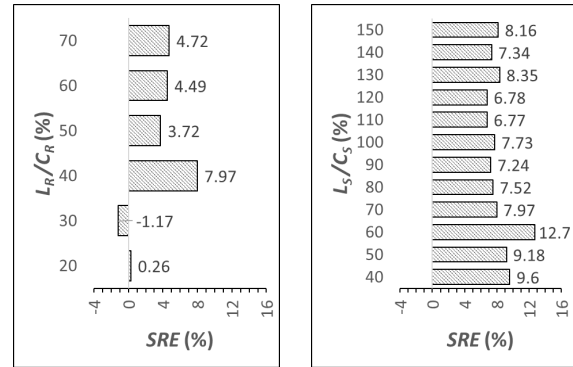
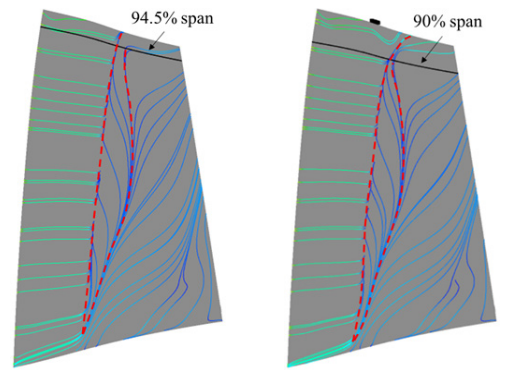
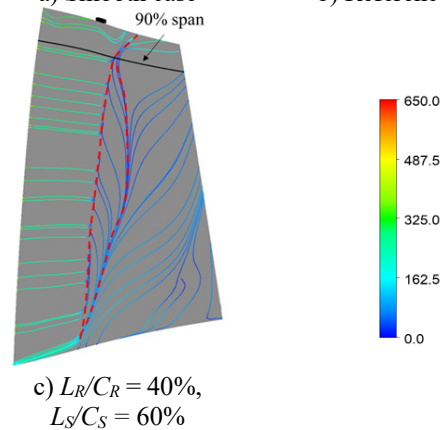


Fig. 7. Effect on operating range



a) Smooth case b) Reference case



c) $L_R/C_R = 40\%$,
 $L_S/C_S = 60\%$

Fig. 8. Streamline on rotor blade suction surface at near-stall (unit: m/s)

On the rotor suction surface (Fig.8), the recirculation region (between the two dashed lines) was reduced in size as the flow separation line was bent downstream, and the reattachment line was contained to the 90 percent span (Fig.8 (b, c)). This delayed the stall, therefore, increased the operating range of the compressor (Fig.7). In the case of $L_R/C_R = 40\%$ and $L_S/C_S = 60\%$, the separation line was bent more backwards near the tip than in the reference case, which is consistent with the increase by 12.7% in the operating range in Fig. b.

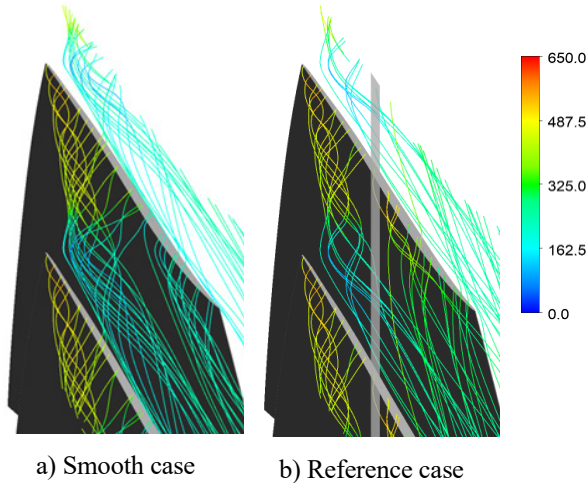


Fig. 9. Rotor tip vortex at near-stall (unit: m/s)

Figure 9 shows a reduction in rotor-tip vortex flow at near-stall condition. In the smooth case (Fig.10a), the streamlines are concentrated around the core of the leakage vortex, whereas in the reference case (Fig.9b), they are distributed evenly on the casing circumference.

4. Conclusion

In this study, the effects of circumferential recirculation channel on a transonic axial compressor have been examined using the $k-\varepsilon$ turbulence model to solve 3D RANS equations. The positions of the bleed and injection ports were changed along the compressor shroud. In general, the results showed that the stall margin and operating range of the compressor were extended by between 0.66% and 2.38%, and between 0.26% and 12.70%, respectively, as a result of the reduction in rotor-tip leakage vortex and the decreased size of the recirculation region on the rotor suction surface at near-stall condition. However, the adiabatic efficiency penalty was high (between 0.43% and 0.66%) due to losses in the channel. The pressure ratios at both operating and near-stall conditions, on the other hand, decreased marginally (less than 1%).

In future work, the bleed port would be considered placed further downstream on high-pressure stages to increase the driving pressure difference between the bleed and injection ports. The installation of mechanical support that connects the channel with the compressor casing would also be studied to apply the concept into reality.

Acknowledgments

This study is funded by the Vietnam National Foundation for Science and Technology Development under grant number 107.03-2018.20.

References

- [1] Kim, J. H., Kim, K. Y., and Cha, K. H., 2013, Effects of Number of Circumferential Casing Grooves on Stall Flow Characteristics of a Transonic Axial Compressor, *Applied Mechanics and Materials*, Vols. 284-287, pp 727–732.
- [2] Wu, Y., Chu, W., Zhang, H., and Li, Q., 2010, Parametric Investigation of Circumferential Grooves on Compressor Rotor Performance, *Journal of Fluids Engineering*, Vol. 132, 121103.
- [3] Kim, J. H., Choi, K. J., and Kim, K. Y., 2013, Aerodynamic analysis and optimization of a transonic axial compressor with casing grooves to improve operating stability, *Aerospace Science and Technology*, Vol. 29(1), pp 81–91.
- [4] Kim, D. W., Kim, J. H., and Kim, K. Y., 2013, Aerodynamic Performance of an Axial Compressor with a Casing Groove Combined with Injection, *Transactions of the Canadian Society for Mechanical Engineering*, Vol. 37, No. 3, pp 283–292.
- [5] Kim, J. H., Kim, D. W., and Kim, K. Y., 2013, Aerodynamic Optimization of a Transonic Axial Compressor with a Casing Groove combined with Tip Injection, *Proceedings of the Institution of Mechanical Engineers, Part A: Journal of Power and Energy*, Vol. 227(8), pp 869–884.
- [6] Weichert, S., Day, I., and Freeman, C., 2011, Self-Regulating Casing Treatment for Axial Compressor Stability Enhancement, *Proceedings of ASME Turbo Expo 2011*, GT2011-46042.
- [7] Strazisar, A.J., Bright, M.M., Thorp, S., Culley, D.E., and Suder, K.L., 2004, Compressor Stall Control Through Endwall Recirculation, *Proceedings of ASME Turbo Expo 2004*, GT2004-54295.
- [8] Hathaway, M.D., 2002, Self-Recirculating Casing Treatment Concept for Enhanced Compressor Performance, *Proceedings of ASME Turbo Expo 2002*, GT2002-30368.
- [9] Dinh, C.T., Ma, S.B., and Kim, K.Y., Aerodynamic Optimization of a Single-Stage Axial Compressor with Stator Shroud Air Injection, *AIAA Journal* 2017, Vol. 55, No. 8, pp 2739–2754.

- [10] Dinh, C. T., Ma, S. B., and Kim, K. Y., 2017, Effects of a Circumferential Feed-Back Channel on Aerodynamic Performance of a Single-Stage Transonic Axial Compressor, In Proceedings of ASME Turbo Expo 2017, GT2017-63536.
- [11] Reid, L., and Moore, R. D., 1987, Design and Overall Performance of Four Highly Loaded, High-Speed Inlet Stages for an Advanced High-Pressure_Ratio Core Compressor, NASA Technical Paper 1337, Lewis Research Center, Cleveland, Ohio 44135.
- [12] ANSYS CFX-19.1, 2018, ANSYS Inc.,
- [13] Launder, B. E., and Spalding, D. B., 1983, The Numerical Computation of Turbulent Flows, Numerical Prediction of Flow, Heat Transfer, Turbulence and Combustion, pp 96–116.